

## P<sup>3</sup>-[2-(4-hydroxyphenyl)-2-oxo]ethyl ATP for the Rapid Activation of the Na<sup>+</sup>,K<sup>+</sup>-ATPase

Sven Geibel,\* Andreas Barth,<sup>†</sup> Sabine Amslinger,<sup>‡</sup> Andreas H. Jung,<sup>‡</sup> Christiane Burzik,\* Ronald J. Clarke,\* Richard S. Givens,<sup>‡</sup> and Klaus Fendler\*

\*Max-Planck-Institut für Biophysik, D-60596 Frankfurt/Main, Germany; <sup>†</sup>Institut für Biophysik, Johann Wolfgang Goethe-Universität, D-60590 Frankfurt/Main, Germany; and <sup>‡</sup>Department of Chemistry, University of Kansas, Lawrence, Kansas 66045 USA

**ABSTRACT** P<sup>3</sup>-[2-(4-hydroxyphenyl)-2-oxo]ethyl ATP (pHP-caged ATP) has been investigated for its application as a phototrigger for the rapid activation of electrogenic ion pumps. The yield of ATP after irradiation with a XeCl excimer laser ( $\lambda = 308$  nm) was determined at pH 6.0–7.5. For comparison, the photolytic yields of P<sup>3</sup>-[1-(2-nitrophenyl)]ethyl ATP (NPE-caged ATP) and P<sup>3</sup>-[1,2-diphenyl-2-oxo]ethyl ATP (desyl-caged ATP) were also measured. It was shown that at  $\lambda = 308$  nm pHP-caged ATP is superior to the other caged ATP derivatives investigated in terms of yield of ATP after irradiation. Using time-resolved single-wavelength IR spectroscopy, we determined a lower limit of  $10^6$  s<sup>-1</sup> for the rate constant of release of ATP from pHP-caged ATP at pH 7.0. Like NPE-caged ATP, pHP-caged ATP and desyl-caged ATP bind to the Na<sup>+</sup>,K<sup>+</sup>-ATPase and act as competitive inhibitors of ATPase function. Using pHP-caged ATP, we investigated the charge translocation kinetics of the Na<sup>+</sup>,K<sup>+</sup>-ATPase at pH 6.2–7.4. The kinetic parameters obtained from the electrical measurements are compared to those obtained with a technique that does not require caged ATP, namely parallel stopped-flow experiments using the voltage-sensitive dye RH421. It is shown that the two techniques yield identical results, provided the inhibitory properties of the caged compound are taken into account. Our results demonstrate that under physiological (pH 7.0) and slightly basic (pH 7.5) or acidic (pH 6.0) conditions, pHP-caged ATP is a rapid, effective, and biocompatible phototrigger for ATP-driven biological systems.

### INTRODUCTION

A variety of caged ATP derivatives have been used for the investigation of ion transport and muscle contraction. The most widely used compound is P<sup>3</sup>-[1-(2-nitrophenyl)ethyl] ester of ATP (NPE-caged ATP) (Kaplan et al., 1978). This caged ATP has also been used in the study of charge translocation in a number of ion-translocating membrane proteins (for a review see Fendler et al., 1998). A prominent member of this group is Na<sup>+</sup>,K<sup>+</sup>-ATPase, which is present in virtually every mammalian cell. This enzyme transports three Na<sup>+</sup> ions out of the cell and two K<sup>+</sup> ions into the cell at the expense of the hydrolytic energy of one ATP molecule. Early investigations demonstrated that NPE-caged ATP bound to the Na<sup>+</sup>,K<sup>+</sup>-ATPase and acted as a competitive inhibitor (Forbush, 1984). Because of the inhibitory action of NPE-caged ATP, ATP binding was slowed down appreciably to relaxation rates on the order of 30 s<sup>-1</sup> (Fendler et al., 1993). However, this did not hinder the determination of rate constants of processes much greater than 30 s<sup>-1</sup>, because it was found that ATP binding and the subsequent reactions occur in different phases of the electrical signal measured after photolytic activation of Na<sup>+</sup>,K<sup>+</sup>-ATPase (Fendler et al., 1987, 1993).

A more serious drawback of NPE-caged ATP is its slow release under physiological conditions ( $\tau^{-1} \approx 86$  s<sup>-1</sup> at pH 7.05, 4 mM Mg<sup>2+</sup> and 24°C; Gropp et al., 1999; Walker et al., 1988; Barabas and Keszthelyi, 1984). For this reason most measurements were performed under slightly acidic conditions (pH 6.2, 3 mM Mg<sup>2+</sup>, and 24°C; Fendler et al., 1993), where the relaxation rate for ATP release is  $\sim 1000$  s<sup>-1</sup>. An additional desirable property of a caged ATP is its biocompatibility. In some cases, NPE-caged ATP has been shown to inactivate Na<sup>+</sup>,K<sup>+</sup>-ATPase at high concentrations, primarily because of the reactive photoproducts accompanying the release of ATP. Fortunately this effect can be greatly reduced by the addition of glutathione as a scavenger (Kaplan et al., 1978). No inactivation of the Na<sup>+</sup>,K<sup>+</sup>-ATPase was found in bilayer measurements, possibly because of the lower concentrations employed in these studies (Fendler et al., 1985; Borlinghaus et al., 1987).

Several other caged ATP compounds have been developed 1) to maximize the yield of ATP, 2) to increase the rate of release of ATP at physiological pH, and 3) to improve its biocompatibility. One of these, the P<sup>3</sup>-[1-(3, 5-dimethoxyphenyl)-2-phenyl-2-oxo]ethyl ester of ATP (DMB-caged ATP) (Thirlwell et al., 1994) was found to release ATP under physiological conditions at a rate that was fast enough for this study. However, the yield of ATP from irradiation of DMB-caged ATP with a frequency-doubled ruby laser ( $\lambda = 347$  nm) was rather poor (nearly 10 times less than with NPE-caged ATP) because of a low extinction coefficient at 347 nm (Sokolov et al., 1998; Thirlwell et al., 1994). A low yield of ATP from DMB-caged ATP was also found by using irradiation from a flashlight (<7%; Sokolov et al.,

Received for publication 24 January 2000 and in final form 8 June 2000.

Address reprint requests to Dr. Klaus Fendler, Max-Planck-Institut für Biophysik, Kennedyallee 70, D-60596 Frankfurt/Main, Germany. Tel.: 49-69-6303-306; Fax: +49-69-6303-305; E-mail: fendler@mpibp-frankfurt.mpg.de.

© 2000 by the Biophysical Society

0006-3495/00/09/1346/12 \$2.00

1998). In this case, DMB-caged ATP was only slightly less effective than NPE-caged ATP (Sokolov et al., 1998).

A very powerful and convenient light source for these studies is a XeCl excimer laser ( $\lambda = 308$  nm). The recently introduced  $P^3$ -[2-(4-hydroxyphenyl)-2-oxo]ethyl ATP (pHP-caged ATP) was expected to release ATP very efficiently, with the use of a XeCl excimer laser, because of its high extinction coefficient at 308 nm. In addition, it appeared to be well suited to the physiological range desired, based on the reported efficiency and rate of release of ATP (Park and Givens, 1997; Givens et al., 1998). Here we report the properties of pHP-caged ATP, with emphasis on its applicability to the study of charge translocation of  $Na^+, K^+$ -ATPase. We demonstrate that pHP-caged ATP is biocompatible and, using 308-nm radiation, that it releases ATP in higher yield than  $P^3$ -[1,2-diphenyl-2-oxo]ethyl ATP (desyl-caged ATP) or NPE-caged ATP and with a much larger rate constant than NPE-caged ATP under the physiological conditions used in our studies. To show that correct kinetic information is obtained with this new phototrigger, we undertake a kinetic analysis of the  $Na^+, K^+$ -ATPase based on the measurement of transient currents after activation with pHP-caged ATP.

With the prospect of a more rapid, highly efficient release of ATP from pHP-caged ATP, we were able to explore fast processes that occur with  $Na^+, K^+$ -ATPase over a broad pH range, including a physiological pH range that was not accessible with NPE-caged ATP. This allowed the kinetic analysis of rapid reactions in the reaction cycle of the  $Na^+, K^+$ -ATPase at a physiological pH heretofore unapproachable with the NPE-caged derivatives.

Therefore, this study may help to resolve a long-standing controversy concerning the rate constant of a conformational transition (the  $E_1P \rightarrow E_2P$  transition) in the reaction cycle of the  $Na^+, K^+$ -ATPase. For this reaction, values ranging from  $29 s^{-1}$  (Stürmer et al., 1991) to  $1400 s^{-1}$  (Hobbs et al., 1985; Fendler et al., 1993) have been reported. Comparison of the rate constants has always been hampered by the fact that the measurements, which yielded conflicting values, were performed under different conditions, i.e., at different pH values, ionic strengths, temperatures, and enzyme preparations. Using pHP-caged ATP, we have now determined this rate constant at different pH values but under otherwise identical conditions. We found a lower limit for this rate constant of  $k > 270 s^{-1}$  in the pH range 6.2–7.4. Differing pH values, therefore, cannot account for the diverging results obtained before.

## MATERIALS AND METHODS

### Preparation of the $Na^+, K^+$ -ATPase

Microsomal membranes containing  $Na^+, K^+$ -ATPase were prepared and purified from the red outer medulla of pig kidney as described previously (Jorgensen, 1974a,b). Samples of the material were quickly frozen and

stored in liquid nitrogen before use. The concentration of the enzyme was 2–3 mg/ml; its activity was  $10$ – $15 \mu\text{mol P}_i \text{ min}^{-1} \text{ mg}^{-1}$  at  $24^\circ\text{C}$ .

### Luciferase assay

Luciferase assay (Boehringer Mannheim) was used to determine ATP concentrations in solution as described previously (Fendler et al., 1985). In the range of  $10^{-8}$  to  $10^{-6}$  M ATP, luminescence of the luciferase assay increases linearly with ATP concentration. Thus the ATP concentration in caged ATP probes could be determined through luminescence measurements, provided the ATP concentration was within this concentration range. As a standard,  $10 \mu\text{l}$  of ATP solutions ( $10^{-6}$ ,  $10^{-7}$ ,  $10^{-8}$  M ATP in purified water) were mixed with aliquots containing  $50 \mu\text{l}$  of luciferase assay solution and  $150 \mu\text{l}$  of purified water, and the luminescence was determined. For the determination of an unknown ATP concentration,  $10 \mu\text{l}$  of the sample (caged ATP solution in a buffer of 130 mM NaCl, 3 mM  $MgCl_2$ , 25 mM imidazole at pH 6.0, 6.5, 7.0, and 7.5) was mixed with the same aliquots and the luminescence was determined. This was done 1) before illumination of the sample, 2) after illumination under conditions similar to those for the bilayer measurements in the same cuvette with 30 laser flashes of the typical intensity used for the bilayer measurements ( $150 \text{ mJ/cm}^2$ ), and 3) after repeated illumination with high laser flash intensity, which was sufficient to photolyze all of the caged ATP present.

### Infrared measurements

An aqueous solution of 100 mM pHP-caged ATP, 400 mM imidazole/HCl (pH 7.0), and 100 mM  $MgCl_2$  was placed in demountable  $CaF_2$  cuvettes with a  $5\text{-}\mu\text{m}$  path length for the Fourier transform infrared (FTIR) measurements or an  $8\text{-}\mu\text{m}$  path length for the single-wavelength measurements. Time-resolved FTIR measurements were performed at  $24^\circ\text{C}$  with a modified Bruker IFS 66 spectrometer at  $4 \text{ cm}^{-1}$  resolution as described before. Difference spectra for the time intervals after the photolysis flash were calculated with respect to a single-beam spectrum consisting of 300 interferometer scans recorded immediately before the flash. Single-wavelength kinetics were measured at  $24^\circ\text{C}$  with a dispersive infrared spectrometer as described (Barth et al., 1995). The monochromator slits were set at  $20 \text{ cm}^{-1}$  resolution, and an electronic filter of  $1 \mu\text{s}$  was used. A  $4000 \text{ cm}^{-1}$  cutoff filter (Barth et al., 1995) between the light source and the sample prevented heating of the sample, and a  $2000 \text{ cm}^{-1}$  cutoff filter in front of the detector blocked intensity from higher orders that had passed the monochromator. pHP-caged ATP was photolyzed with a 10-ns excimer laser pulse at 308 nm, which was focused on the infrared cuvette to give  $\sim 80 \text{ mJ}$  per flash on the sample area. The signals of the first flash on five samples were averaged at  $1140 \text{ cm}^{-1}$ . For 1200 and  $1270 \text{ cm}^{-1}$ , two samples were averaged. To quantify the time resolution of the spectrometer, the 32nd order of the laser stray light signal was measured at  $32 \times 308 \text{ nm}$  without the germanium filter in front of the detector.

### Bilayer measurements

Optically black lipid membranes (BLMs) with an area of  $0.01$ – $0.02 \text{ cm}^2$  were formed in a thermostatted Teflon cell as described elsewhere (Fendler et al., 1985). Each of the two compartments of the cell was filled with 1.5 ml of electrolyte containing 130 mM NaCl, 3 mM  $MgCl_2$ , 1 mM dithiothreitol, and 25 mM imidazole at pH 6.2, 7.0, or 7.4. The temperature was kept at  $24^\circ\text{C}$ . The membrane-forming solution contained 1.5% (w/v) diphytanoylphosphatidylcholine (Avanti Polar Lipids, Alabaster, AL) and 0.025% (w/v) octadecylamine (Riedel de Haen, Hannover, Germany) dissolved in *n*-decane.

The membrane was connected to an external measuring circuit via polyacrylamide gel salt bridges and Ag/AgCl electrodes. The signal was amplified, filtered, and recorded with a digital oscilloscope. A first-order,

low-pass filter with a cutoff frequency of 3000 Hz was used. (For further details see Fendler et al. (1985, 1987, 1993).) Pig kidney  $\text{Na}^+, \text{K}^+$ -ATPase membrane fragments and caged ATP were added under stirring to one compartment of the cuvette. To photolyze the caged ATP, light pulses of a XeCl excimer laser ( $\lambda = 308 \text{ nm}$ ) with a duration of 10 ns were attenuated by neutral density filters and focused onto the lipid bilayer membrane. At an energy density of  $\sim 150 \text{ mJ}\cdot\text{cm}^{-2}$ ,  $\sim 26\%$  of the NPE-caged ATP and  $\sim 40\%$  of the pHP-caged ATP are released as ATP by a single light flash. These values were calculated using the parameters given in Table 3.

## Caged compounds

pHP-caged ATP was prepared as described (Park and Givens, 1997). According to 400 MHz H-NMR measurements, the sample of pHP-caged ATP that was used consisted of 71.4% (mass) pHP-caged ATP (MW 692), 3.7% caged  $\text{P}_i$ , and 24.9% inorganic salts. Therefore the concentration of pHP-caged ATP in the sample was  $\sim 970 \text{ mmol/g}$  of the dry probe. The sample was diluted with water to give stock solutions with the appropriate concentration. NPE-caged ATP was purchased from Calbiochem (Bad Soden, Germany). Desyl-caged ATP was purchased from Molecular Probes (Eugene, OR).

## Stopped-flow measurements

Stopped-flow experiments were carried out using an SF-61 stopped-flow spectrofluorimeter from Hi-Tech Scientific (Salisbury, UK) as described elsewhere (Kane et al., 1998). The kinetic data were collected via a high-speed 12-bit analog-to-digital data acquisition board and were analyzed using software developed by Hi-Tech Scientific. Each kinetic trace consisted of 1024 data points. To improve the signal-to-noise ratio, typically 6–14 experimental traces were averaged before the reciprocal relaxation time was evaluated.

The kinetics of the  $\text{Na}^+, \text{K}^+$ -ATPase conformational changes and competitive effects of pHP-caged ATP were investigated in the stopped-flow apparatus by mixing  $\text{Na}^+, \text{K}^+$ -ATPase labeled with the voltage-sensitive dye RH421 in one of the drive syringes with an equal volume of an ATP solution from the other drive syringe in the absence and presence of pHP-caged ATP in either the enzyme or ATP syringe. The two solutions were prepared in the same buffer (130 mM NaCl, 3 mM  $\text{MgCl}_2$ , and 25 mM imidazole at pH 6.2, 7.0, or 7.4). The solutions in the drive syringes were equilibrated to a temperature of  $24^\circ\text{C}$  before each experiment. The traces were fitted with a biexponential function, where the fast rise can be assigned to the kinetics of phosphorylation and the associated conformational change of the  $\text{Na}^+, \text{K}^+$ -ATPase, while the slow phase ( $>50 \text{ ms}$ ) is attributed to the relaxation of the dephosphorylation/rephosphorylation equilibrium in the absence of  $\text{K}^+$  ions (Clarke et al., 1998). Interference of a photochemical reaction of RH421 with the kinetics of the  $\text{Na}^+, \text{K}^+$ -ATPase-related fluorescence transients was avoided by inserting neutral density filters in the light beam in front of the monochromator (Kane et al., 1997). When the fast phase became slow ( $>20 \text{ ms}$ ) because of inhibitory effects of the caged compound on the  $\text{Na}^+, \text{K}^+$ -ATPase, it was found that the traces could be fitted by a monoexponential function.

## Reagents

The following quality of reagents was used: imidazole, 99%+ (Sigma) or  $\geq 95\%$  (Fluka); NaCl, Suprapur (Merck);  $\text{MgCl}_2\cdot 6\text{H}_2\text{O}$ , analytical grade (Merck); HCl, 0.1 N Titrisol solution (Merck); dithiothreitol, 95% (Reanal, Budapest), ATP disodium salt $\cdot 3\text{H}_2\text{O}$ , special quality (Boehringer Mannheim); ethanol, analytical grade (Merck).

## RESULTS

The principal issue of the present study is the characterization of a novel phototrigger for ATPases, pHP-caged ATP.

We have used the luciferase assay and FTIR spectroscopy as well as electrical measurements and stopped-flow fluorescence spectroscopy on  $\text{Na}^+, \text{K}^+$ -ATPase to determine the properties of this compound and to demonstrate its suitability for the investigation of charge transport by ATP-driven membrane proteins. For comparison, we have also carried out a limited investigation of two commercially available compounds, NPE-caged and desyl-caged ATP. NPE-caged and desyl-caged ATP were studied using the luciferase assay. Desyl-caged ATP was also tested in electrical measurements on the  $\text{Na}^+, \text{K}^+$ -ATPase. The latter data are not shown and are only briefly mentioned in the Discussion. Electrical measurements using NPE-caged ATP have been published previously. The chemical structures of the three caged compounds are shown in Fig. 1.

## Luciferase assay

Using a 1 mM stock solution, a caged ATP concentration in the cuvette was prepared that yielded a concentration of released ATP in the measurable range ( $10^{-8}$  to  $10^{-6} \text{ M}$ ). Then the photochemically released fraction  $\eta$  of ATP from pHP-caged ATP was determined after laser irradiation (308 nm). At the typical laser flash intensity of  $150 \text{ mJ}\cdot\text{cm}^{-2}$  the fraction of photochemically released ATP was shown to be  $\sim 40\%$  per laser flash. When the sample was photolyzed to full conversion, the fraction of released ATP did not exceed  $\sim 75\%$ . The reason for the incomplete photochemi-

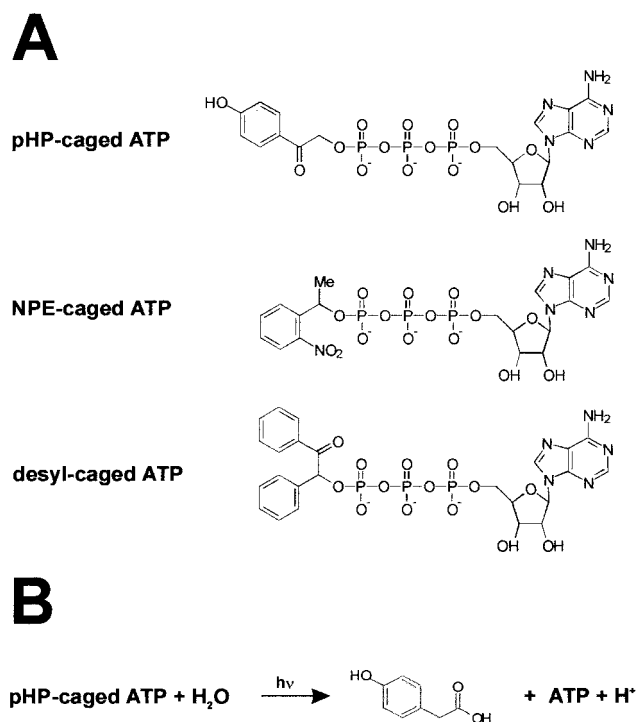


FIGURE 1 (A) Caged ATPs: chemical structures. (B) Photolytic release of ATP from pHP-caged ATP

cal product yield is not clear. A similar fraction of released ATP after prolonged irradiation has been reported for NPE-caged ATP (Kaplan et al., 1978).

### Infrared measurements

Time-resolved infrared spectral changes with a time resolution of 60 ms were recorded with an FTIR spectrometer. The changes in molecular structure upon photolysis of pHP-caged ATP are reflected in the infrared absorbance changes that, in principle, can be used to measure the rate of caged ATP photolysis. By taking the difference of the absorbance after photolysis minus the absorbance before photolysis, we obtained the calculated infrared difference spectrum (Fig. 2 A). Negative bands are characteristic of the educts, and positive bands, of the products of the photolysis reaction. For the spectrum in Fig. 2 A, the absorbance spectra after photolysis were recorded in the time interval of 10 ms to 11 s after the light flash.

Because it has been established in earlier studies that the phosphate bands can be used to measure the rate of ATP release for NPE-caged ATP (Barth et al., 1995, 1997), the two main phosphate marker bands at 1129 and 1270  $\text{cm}^{-1}$  (see Fig. 2 A) were monitored during the photolysis. The release of ATP transforms the covalently attached pHP- $\text{PO}_2^-$  group into the  $\gamma\text{-PO}_3^{2-}$  group of ATP, which is accompanied by a decrease in electron density in the P-O bonds. It is therefore reflected in the shift of a caged ATP  $\text{PO}_2^-$  band at 1270  $\text{cm}^{-1}$  to one at 1129  $\text{cm}^{-1}$ , which is assigned to the broad  $\gamma\text{-PO}_3^{2-}$  band of free ATP. This is discussed in more detail in Barth et al. (1995) and Barth et al. (1997). The band positions obtained here are slightly different from those found for NPE-caged ATP (1251 and 1119  $\text{cm}^{-1}$ ; Barth et al., 1995) because  $\text{Mg}^{2+}$  is present in the experiments shown here. If pHP-caged ATP is photolyzed in the absence of  $\text{Mg}^{2+}$ , the bands are found at 1257 and 1125  $\text{cm}^{-1}$  (data not shown), i.e., closer to the respec-

tive bands of NPE-caged ATP. The remaining small discrepancy in band position between pHP-caged ATP and NPE-caged ATP may be due to bands that are characteristic of the photolysis educts that are different for the two caged derivatives (discussed below).

Infrared difference bands of groups other than the phosphates will be discussed only briefly here (data not shown). In line with the proposed mechanism (Park and Givens, 1997), bands that may be attributed to the disappearing keto group and to the antisymmetrical and symmetrical stretching vibrations of the appearing carboxylate group of the photolysis product *p*-hydroxyphenylacetic acid (Fig. 1 B) are observed at 1686 (-), 1556 (+), and 1390  $\text{cm}^{-1}$  (+), respectively. Other bands at 1606 (-), 1585 (-), 1517 (+), and 1505  $\text{cm}^{-1}$  (-) show the perturbation of the ring system, with the latter two indicating a band shift due to the lower electron-withdrawing capacity of the product substituent (Colthup et al., 1975). The shift is due to the insertion of a methylene group between the carbonyl of the *p*-hydroxyacetophenone group and the ring during the photorearrangement of the cage to yield a phenylacetic acid.

As expected for the photolysis product *p*-hydroxyphenylacetic acid (Fig. 1 B), the generation of an acidic proton in the photorearrangement could be detected at pH 7.0 when the buffer *N*-(2-acetamido)-iminodiacetic acid-KOH (ADA) was used. This compound buffers with carboxyl groups that give strong infrared signals at 1581 (-), 1625 (+), and 1704  $\text{cm}^{-1}$  (+) upon protonation (Hauser, 1994). These signals (data not shown) appeared upon pHP-caged ATP photolysis within the time resolution of the experiment (the duration of recording the first spectrum was 60 ms).

The time resolution of 60 ms of the FTIR measurements proved to be too slow to resolve the release of ATP. Therefore single-wavelength measurements were made at selected difference bands with a dispersive infrared spectrometer. These are shown in Fig. 2 B. The kinetic measurements of ATP release were not made at the local maximum of the

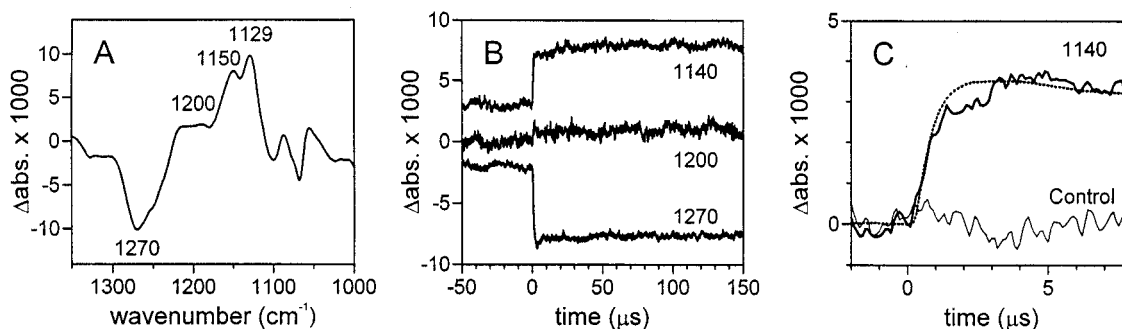


FIGURE 2 Infrared measurements of ATP release from pHP-caged ATP. (A) FTIR difference spectrum of pHP-caged ATP photolysis at 24°C. The absorbance recorded 10 ms to 11 s after the photolysis flash minus the absorbance immediately before the photolysis flash was calculated. (B) Infrared absorbance changes at 1270, 1200, and 1140  $\text{cm}^{-1}$  upon photolysis of pHP-caged ATP measured at 24°C with a dispersive infrared spectrometer. A constant value was added to the traces recorded at 1140 and 1270  $\text{cm}^{-1}$  for a clearer presentation. (C) Infrared absorbance change at 1140  $\text{cm}^{-1}$  shown on a shorter time scale after subtraction of the smoothed 1200  $\text{cm}^{-1}$  signal. Bold line: ATP release signal (first flash). Thin line: heat signal (second flash without measuring light). Dotted line: integrated signal of the laser excitation flash normalized to the maximum of the 1140  $\text{cm}^{-1}$  signal.

$\text{PO}_3^{2-}$  band at  $1129\text{ cm}^{-1}$ , but rather at the center of this broad band at  $1140\text{ cm}^{-1}$  (resolution  $20\text{ cm}^{-1}$ ). As expected from the FTIR difference spectra, a positive signal at  $1140\text{ cm}^{-1}$ , a strong negative signal at  $1270\text{ cm}^{-1}$ , and a very small positive signal at  $1200\text{ cm}^{-1}$  were observed in the kinetic measurements. The latter serves as a control measurement to quantify possible artifacts.

The signal monitoring the production of free ATP at  $1140\text{ cm}^{-1}$  showed a step change in the first few microseconds and a further slight increase in the following  $50\ \mu\text{s}$ . The latter was also present in the kinetic traces of the other two bands, although this was less apparent at first. If, however, the data are averaged in the time intervals of  $5\text{--}50\ \mu\text{s}$  and  $100\text{--}150\ \mu\text{s}$ , then all traces show an increase in absorbance of  $0.2\text{--}0.4 \times 10^{-3}$  absorbance units. This increase is also detected in all three traces if the data are smoothed between  $5$  and  $150\ \mu\text{s}$ . This uniform behavior of the slow process makes its attribution to the kinetics of the initial photorelease of substrate in the photolysis reaction unlikely.

The slower process is also observed when a frequency-tripled Nd-Yag laser at  $355\text{ nm}$  is used for excitation. At this wavelength, the photolysis yield of ATP from pHP-caged ATP is low, and the signal is dominated by the slow process that appears over a wide wavenumber range. Thus we attribute the slow process to an artifact signal, probably generated by a transient absorbance change of water due to the energy absorbed in the sample (Yuzawa et al., 1994). To eliminate the artifact, we subtracted the smoothed (over  $1\ \mu\text{s}$ ) control signal at  $1200\text{ cm}^{-1}$  from the ATP release signal at  $1140\text{ cm}^{-1}$ , thus effectively making a two-wavelength measurement. Fig. 2 C shows the corrected ATP release signal at  $1140\text{ cm}^{-1}$  on a shorter time scale. It is evident that the signal corresponding to ATP release rises with a time constant of  $\sim 1\ \mu\text{s}$ .

Also shown (Fig. 2 C, *dotted line*) is the integrated stray light signal of the 10-ns XeCl laser pulse corresponding to the total light energy accumulated in the sample. The rise time of this signal is limited by the time constants of the detector and the electronics. Comparing the ATP release signal and the integrated laser light signal, it is clear that the two are coincident. Thus a lower limit for the relaxation rate of ATP release can be given here as at least  $10^6\text{ s}^{-1}$  at  $24^\circ\text{C}$ .

Fig. 2 C also shows a control signal that was recorded using the second flash on the same sample while the infrared measuring light was switched off. This demonstrates the absence of a heat radiation signal due to increased infrared radiation upon transient heating of the sample (not to be confused with the artifact due to a transient water absorbance change). The third flash (not shown) was again recorded with the infrared measuring light switched on. It produced a signal identical to that from the first flash but with only 40% signal intensity.

## Current measurements

$\text{Na}^+, \text{K}^+$ -ATPase-containing membrane fragments were adsorbed on the BLM as described in Materials and Methods.

Using pHP-caged ATP, it is possible to generate a rapid ATP concentration jump by illumination of the compound membrane with a UV laser flash. The released ATP activates the  $\text{Na}^+, \text{K}^+$ -ATPase contained in the adsorbed membrane fragments, and a transient current can be measured. This signal reflects charge transport during the early,  $\text{Na}^+$ -dependent step of the reaction cycle (Fendler et al., 1985). Repetitive flashing of the sample under identical conditions yielded identical signals. This shows that pHP-caged ATP is biocompatible, i.e., it does not inactivate the  $\text{Na}^+, \text{K}^+$ -ATPase after many ( $>50$ ) illuminations.

Because the release of ATP from pHP-caged ATP occurs rapidly not only under acidic but also under neutral or alkaline conditions, the  $\text{Na}^+, \text{K}^+$ -ATPase could be investigated at pH values of 6.2, 7.0, and 7.4. First the concentration of pHP-caged ATP was varied, then the laser flash intensity was decreased as described in Materials and Methods. Current traces obtained at different pH values are shown in Fig. 3 together with a fit based on the kinetic model described later. In the absence of any ionophores the pump current is capacitively coupled to the measuring system. Under these conditions the electrical current measured after the photolytic release of ATP is characterized by three phases: a rapid rise ( $200\text{--}400\text{ s}^{-1}$ ), a slower decay ( $30\text{--}60\text{ s}^{-1}$ ), and a very slow component ( $\sim 5\text{ s}^{-1}$ ) with negative amplitude, which can be assigned to the system time constant (Fendler et al., 1993). The system time constant represents discharge of the capacitances of planar membrane and liposomes and is determined by their passive electrical properties. No information about the  $\text{Na}^+, \text{K}^+$ -ATPase may be obtained from the value of the system time constant. However, from the amplitude of the negative phase decaying with the system time constant, the magnitude of the stationary current generated by the ion pump can be determined (Fendler et al., 1993).

The peak currents obtained at different pHP-caged ATP concentrations and different pH values are shown in Fig. 4 (*filled symbols*). The peak current increases with rising concentration of pHP-caged ATP, reaches a saturation level, but then decreases at high concentrations of pHP-caged ATP. Note that a direct comparison of the magnitude of the peak currents at different pH values is difficult because each trace is a different experiment that may differ from the others by the amount of adsorbed membrane fragments.

One possible explanation for the decrease in the peak current at high concentrations of pHP-caged ATP could be the inhibitory effects of contaminants in the pHP-caged ATP solution. When the concentration of the caged ATP is increased, more of the contaminant is also introduced, leading to an increased inactivation of the enzyme. From the preparation history of the pHP-caged ATP, we know that these contaminants are  $\text{P}_i$ , caged  $\text{P}_i$ , and  $\text{NH}_4\text{HCO}_3$ . However, control measurements with added  $\text{P}_i$  and  $\text{NH}_4\text{Cl}/\text{NaHCO}_3$  did not show a similar inhibitory effect. Furthermore, the photolytic release of caged  $\text{P}_i$  is not expected to

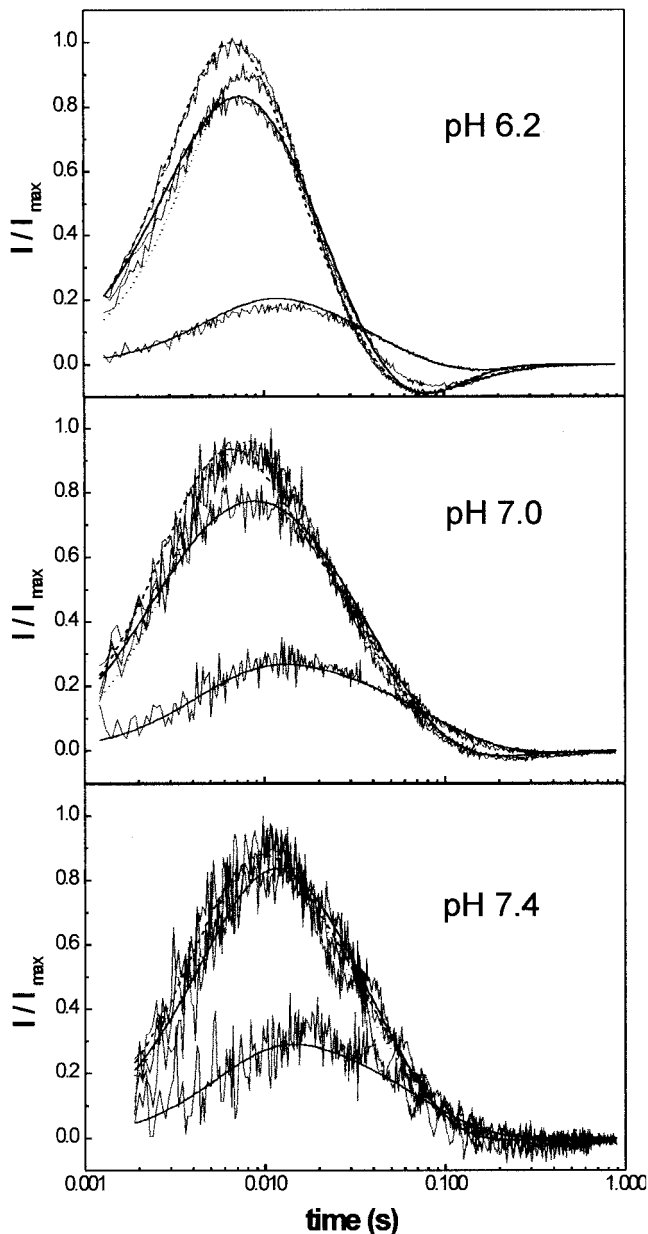


FIGURE 3 Electrical currents after activation of the  $\text{Na}^+, \text{K}^+$ -ATPase, using different concentrations of pHP-caged ATP (10, 30, 100, 300  $\mu\text{M}$ ), at pH 6.2, 7.0, and 7.4. Current traces at the same pH were fitted simultaneously for the four concentrations of pHP-caged ATP according to the kinetic model given in Fig. 7. The parameters obtained by the fit are given in Table 4. The noisy traces are the electrical recordings, the smooth ones are the fit. The fit curves correspond to the following concentrations of caged ATP: 10  $\mu\text{M}$ , solid line, smallest amplitude; 30  $\mu\text{M}$ , dotted line; 100  $\mu\text{M}$ , dashed line; 300  $\mu\text{M}$ , solid line.

contribute to the electrical signal, because binding of  $\text{P}_i$  to the  $\text{Na}^+, \text{K}^+$ -ATPase in the presence of  $\text{Na}^+$  is very slow ( $\tau > 10$  s; Cornelius et al., 1998). A further possibility is a slow dissociation of bound pHP-caged ATP from  $\text{Na}^+, \text{K}^+$ -ATPase, as outlined in the discussion. We propose that the

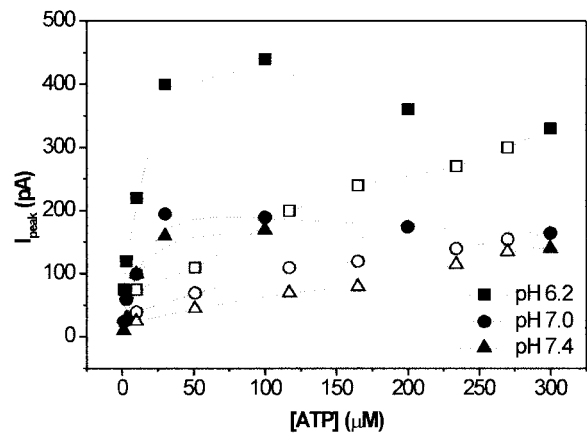


FIGURE 4 ATP dependence of the peak currents generated by the  $\text{Na}^+, \text{K}^+$ -ATPase at different concentrations of released ATP. The peak currents were recorded at different pH:  $\blacksquare, \square$ , pH 6.2;  $\bullet, \circ$ , pH 7.0;  $\blacktriangle, \triangle$ , pH 7.4. The filled symbols represent currents recorded at various pHP-caged ATP concentrations at constant laser flash energy (150 mJ = 40% ATP released from pHP-caged ATP). The open symbols represent currents recorded at constant pHP-caged ATP concentration (300  $\mu\text{M}$ ) but at variable laser flash energies to obtain the different concentrations of released ATP indicated.

slow dissociation of pHP-caged ATP from  $\text{Na}^+, \text{K}^+$ -ATPase causes the decrease in the peak current. This is supported by stopped-flow experiments (see Discussion).

Variation in the laser flash intensity at a constant concentration of pHP-caged ATP (300  $\mu\text{M}$ ) changes the peak current as shown in Fig. 4 (*open symbols*). Compared with measurements with changing pHP-caged ATP concentration, the peak current for the same ATP concentrations was lower in the presence of high pHP-caged ATP concentrations and low light intensity than in the presence of low pHP-caged ATP concentrations and high light intensity. This can be explained by inhibitory effects of pHP-caged ATP and a slow dissociation of pHP-caged ATP from the  $\text{Na}^+, \text{K}^+$ -ATPase (see Discussion).

### Stopped-flow measurements

For comparison with the electrical measurements we determined the rate constants of partial reactions in the  $\text{Na}^+$ -dependent part of the reaction cycle of the  $\text{Na}^+, \text{K}^+$ -ATPase, using stopped-flow fluorescence measurements with the dye RH421. The measurements were performed at various ATP concentrations (final concentrations 10, 30, 100, 300  $\mu\text{M}$  ATP) as described previously (Kane et al., 1997). A typical result obtained after mixing of a solution containing  $\text{Na}^+, \text{K}^+$ -ATPase with a solution containing 100  $\mu\text{M}$  ATP is shown in Fig. 5. The ATP dependence of the relaxation time was determined and analyzed using a hyperbolic fitting function. This yielded half-saturation concentrations for ATP activation ( $K_a$ ) and limiting reciprocal relaxation times ( $k_{\text{max}}$ ) at pH 6.2, 7.0, and 7.4, as shown in Table 1. The

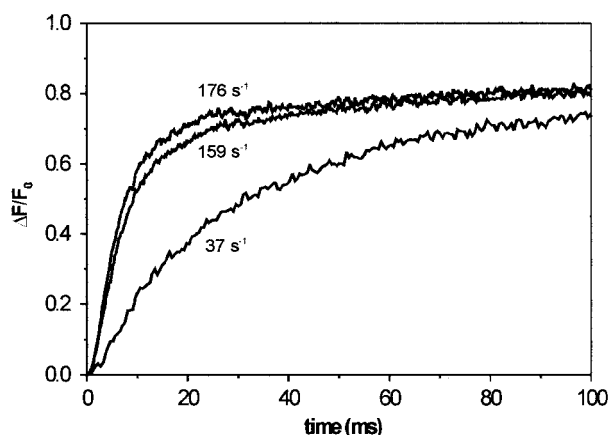


FIGURE 5 Fluorescence change using the potential-sensitive dye RH421 when different  $\text{Na}^+, \text{K}^+$ -ATPase-containing solutions (syringe 1) are mixed with different solutions containing ATP (syringe 2). (a) Syringe 1:  $\text{Na}^+, \text{K}^+$ -ATPase; syringe 2: ATP (100  $\mu\text{M}$ ). (b) Syringe 1:  $\text{Na}^+, \text{K}^+$ -ATPase; syringe 2: ATP (100  $\mu\text{M}$ ) + pHP-caged ATP (100  $\mu\text{M}$ ). (c)  $\text{Na}^+, \text{K}^+$ -ATPase + pHP-caged ATP (100  $\mu\text{M}$ ); syringe 2: ATP (100  $\mu\text{M}$ ). The traces were fitted with exponential functions from which the following relaxation rates were obtained: (a) 176  $\text{s}^{-1}$ ; (b) 159  $\text{s}^{-1}$ ; (c) 37  $\text{s}^{-1}$ .

reciprocal relaxation time  $k_{\text{max}}$  corresponds to an effective rate constant for the two-step reaction  $\text{E}_1\text{ATP} \rightarrow \text{E}_1\text{P} \rightarrow \text{E}_2\text{P}$  (Kane et al., 1997). The values for  $k_{\text{max}}$  and  $K_a$  are in reasonable agreement with previous studies (Fendler et al., 1993; Kane et al., 1997; Clarke et al., 1998). A somewhat lower value of  $k_{\text{max}}$  of  $\sim 90 \text{ s}^{-1}$  was previously reported at pH 6.2 by Kane et al. (1997), but it has since been found that this value was in fact artificially low because of a decrease in pH arising from the added ATP.

### ATP concentration jump in the presence of pHP-caged ATP

To investigate the inhibitory effect of pHP-caged ATP, stopped-flow measurements in the presence of pHP-caged ATP were made. At pH 6.2, 7.0, and 7.4,  $\text{Na}^+, \text{K}^+$ -ATPase-containing membrane fragments and RH421 (syringe 1) were mixed rapidly with ATP (final concentration 100  $\mu\text{M}$ ) and pHP-caged ATP (final concentration 100  $\mu\text{M}$ , syringe 2). The change in fluorescence is shown in Fig. 5. The traces obtained in the absence and presence of pHP-caged ATP in the ATP syringe (labeled 176  $\text{s}^{-1}$  and 159  $\text{s}^{-1}$ , respectively), are nearly identical, and the relaxation times are similar (Table 2).

TABLE 1 Stopped-flow fluorimetric measurements: parameters of a hyperbolic fit to the ATP dependence of the relaxation times

pH	6.2	7.0	7.4
$k_{\text{max}}$ ( $\text{s}^{-1}$ )	156	189	194
$K_a$ ( $\mu\text{M}$ )	6.8	7.4	7.0

TABLE 2 Stopped-flow fluorimetric measurements: reciprocal relaxation times determined in the absence and presence of pHP-caged ATP and after preincubation with pHP-caged ATP

pH	6.2	7.0	7.4
$\tau^{-1}$ ( $\text{s}^{-1}$ )	140	176	186
$\tau^{-1}$ ( $\text{s}^{-1}$ ) + 100 $\mu\text{M}$ caged ATP	133	159	154
$\tau^{-1}$ ( $\text{s}^{-1}$ ) + 100 $\mu\text{M}$ (pre)	55	37	30

In a second stopped-flow experiment, an ATP concentration jump was performed after preincubation of the  $\text{Na}^+, \text{K}^+$ -ATPase with pHP-caged ATP. At pH 6.2, 7.0, and 7.4, pHP-caged ATP (final concentration 100  $\mu\text{M}$ ),  $\text{Na}^+, \text{K}^+$ -ATPase-containing membrane fragments, and RH421 (syringe 1) were rapidly mixed with ATP (final concentration 100  $\mu\text{M}$ , syringe 2). The change in the relative fluorescence is shown in Fig. 5 (labeled 37  $\text{s}^{-1}$ ). It is clear from Fig. 5 that preincubation with pHP-caged ATP drastically slows down the rise of the fluorescence signal. The reciprocal time constant of the fluorescence change based on an ATP concentration jump after preincubation of the  $\text{Na}^+, \text{K}^+$ -ATPase with pHP-caged ATP is much smaller than that obtained from the sample without preincubation with pHP-caged ATP (see Table 2). This behavior is similar to that observed in analogous stopped-flow measurements carried out using NPE-caged ATP (Clarke et al., 1998).

### Analysis of the electrical signals

The recorded currents were fitted using a simplified Albers-Post model (Fig. 7). This model takes into account inhibition of the enzyme by pHP-caged ATP binding. A similar approach has been applied previously to  $\text{Na}^+, \text{K}^+$ -ATPase from eel electric organ and NPE-caged ATP (Fendler et al., 1994). In addition, capacitive coupling of the membrane fragments to the BLM was included as described in Fendler et al. (1993). This introduces the system time constant  $\tau_0$  into the model function. The differential equations describing the kinetic model (see Appendix) were numerically solved and fitted to the data using the software package MLAB (Civilized Software, Bethesda, MD). An essential feature of the procedure is that at a given pH the equations were simultaneously fitted to the currents recorded at four different caged ATP concentrations. Thereby the ATP dependence of the current response was taken into account.

The differential equations and the starting concentrations as well as the calculation of the current are given in the Appendix. The reaction  $\text{E}_2\text{P} \rightarrow \text{E}_1$  comprises several intermediates, but because the decay of  $\text{E}_2\text{P}$  in the absence of  $\text{K}^+$  is slow (4  $\text{s}^{-1}$ ; Hobbs et al., 1985), it can be described with a single rate constant  $k_{21}$ . Two different release models for pHP-caged ATP were tested: 1) Release in site. Caged ATP bound to the  $\text{Na}^+, \text{K}^+$ -ATPase releases ATP after the laser

flash with the same efficiency as in solution. 2) No release in site. Caged ATP bound to the Na<sup>+</sup>,K<sup>+</sup>-ATPase is not photolyzed. Good results were obtained only with the “no release in site” model. Therefore, the model given below was developed using only the latter. Free parameters were the rate constants of pHP-caged ATP binding  $k_c^+$  and dissociation  $k_c^-$ , the rate constant of ATP binding  $k_a^+$ , the rate constant of phosphorylation  $k_p$ , and that of the E<sub>1</sub>P-E<sub>2</sub>P conformational transition  $k_{12}$ , as well as the rate constant of the slow backward reaction  $k_{21}$  and a scaling parameter (which was the same for all four ATP concentrations). The rate constant of ATP dissociation was held constant at  $k_a^- = 50 \text{ s}^{-1}$  (Mardh and Zetterqvist, 1974). The electrogenic step was assumed to be the E<sub>1</sub>P-E<sub>2</sub>P transition (Fendler et al., 1993), and the release of ATP from pHP-caged ATP was assumed to be instantaneous. The back-reaction  $k_{21}$  determines the stationary current. It is reflected in the amplitude of the negative current component and was found to be slow (3–10 s<sup>-1</sup>), which is in accordance with the findings of Hobbs et al. (1985).

When a large number of parameters are being fitted to experimental data, care has to be taken that the information contained in the data is sufficient to determine the parameters unambiguously. Roughly speaking, the number of features of the current traces has to be equal to the number of parameters that are to be determined by the fit. This is indeed the case: the lag and the rising phases of the electrical signal determine  $k_p$  and  $k_{12}$ . The relaxation time of the decay phase, its decrease with rising caged ATP concentration ([caged ATP] < 50 μM), and its increase at high ATP concentrations ([caged ATP] > 50 μM) determine  $k_c^+$ ,  $k_c^-$ , and  $k_a^+$ . The kinetic parameters determined by the fit at the different pH values are compiled in Table 4.

## DISCUSSION

### Efficiency of the photolytic release of ATP

The fraction of released ATP from caged ATP can be calculated by the following equation:

$$1 - \eta = e^{-kE} \quad (1)$$

using the definitions  $\eta$  = fraction of released ATP,  $k$  = release factor (cm<sup>2</sup>/J), and  $E$  = light energy density of the laser flash (J/cm<sup>2</sup>). The fraction of released ATP depends on the release factor  $k$  that was introduced because it is a convenient quantity for the comparison of the efficiency of different caged compounds at a given wavelength. The release factor is related to the quantum efficiency  $q$  by

$$k = \frac{\epsilon q}{h\nu} \quad (2)$$

Here  $\epsilon$  is the molar extinction coefficient at the excitation wavelength and  $h\nu$  is the photon energy. The release factor  $k$  is proportional to the extinction coefficient, which is highly wavelength dependent. However, the quantum efficiency, in general, is not wavelength dependent.

Using the luciferase assay, we determined the fraction  $\eta$  of released ATP from which the release factor  $k$  was obtained using Eq. 1. The quantum efficiency  $q$  was calculated from Eq. 2. The values for the different compounds are compared in Table 3. Note that values for DMB-caged ATP are also given for comparison ( $k$  was calculated according to Eq. 2). The release factor  $k$  is the experimentally relevant quantity for estimating the efficiency of release for a caged compound at a given laser wavelength. The release factor  $k$  for 308-nm XeCl excimer laser irradiation for different caged ATPs and at different pH values is given in Fig. 6 and Table 3. This figure demonstrates the superior performance of pHP-caged ATP under these conditions. As can be seen in Table 3, this is due to the much higher extinction coefficient of pHP-caged ATP at the laser wavelength. The XeCl excimer laser ( $\lambda = 308 \text{ nm}$ ) is a very convenient and powerful light source and has been widely used for photolytic experiments. Good performance at 308 nm is, therefore, an advantage of this pHP-caged compound.

The quantum efficiencies given in the table vary between 0.21 and 0.71, and the extinction coefficients, between 650 and 5800 M<sup>-1</sup>cm<sup>-1</sup>. This underlines the dominant effect of the extinction coefficient for the efficiency of the caged compounds. Although NPE-caged ATP has a higher quantum efficiency than pHP-caged ATP at all pH values measured, pHP-caged ATP is nearly twice as effective because

**TABLE 3** Luciferase assay: comparison of the molar extinction coefficients at  $\lambda = 308 \text{ nm}$ ,  $\epsilon_{308}$  (M<sup>-1</sup>cm<sup>-1</sup>), the release factors  $k$  (cm<sup>2</sup>J<sup>-1</sup>), and the quantum efficiencies  $q$  of different caged ATPs at pH 6.0–7.5

pH	6.0			6.5			7.0			7.5		
	$\epsilon_{308}$	$k$	$q$	$\epsilon_{308}$	$k$	$q$	$\epsilon_{308}$	$k$	$q$	$\epsilon_{308}$	$k$	$q$
pHP	3750	3.5	0.36	4080	3.5	0.33	4470	3.3	0.28	5800	3.2	0.21
NPE	1670	2.1	0.48	1760	1.8	0.39	1730	1.9	0.43	1720	1.4	0.32
desyl	700	0.65	0.36	680	0.85	0.48	660	1.0	0.58	650	1.2	0.71
DMB							940*	0.7 <sup>†</sup>	0.3 <sup>‡</sup>			

\*J. E. T. Corrie, unpublished observation.

<sup>†</sup>Calculated using  $\epsilon_{308}$  and  $q$ .

<sup>‡</sup>Corrie and Trentham (1993).

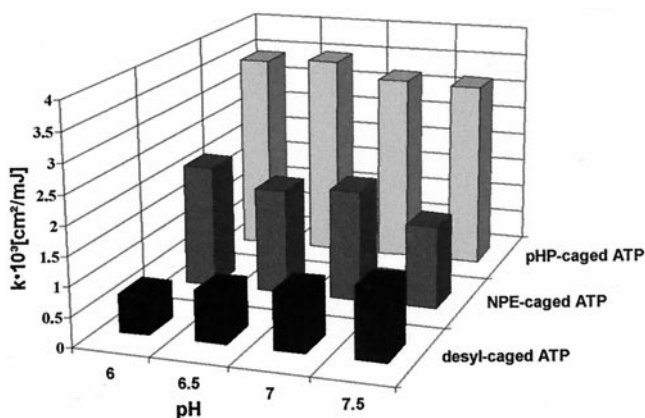


FIGURE 6 Release factor  $k$  of different caged ATPs for XeCl excimer laser irradiation at 308 nm.

of its large absorption coefficient at 308 nm. In the same way, the poor performance of desyl-caged ATP is mainly due to its low absorption coefficient at 308 nm. In the investigated pH region the efficiency of all caged compounds was only slightly pH dependent (Fig. 6). The largest pH effect was found for desyl-caged ATP, which seems to be better at slightly basic pH because of an increased quantum efficiency.

For pHP-caged ATP, Givens and Park (1996) reported a quantum efficiency of 0.3 at pH 7.3, which is consistent with our observation of 0.28 at pH 7.0 but considerably higher than our value of 0.21 at pH 7.5. At pH > 7.0, the increased negative charge associated with the departing triphosphate creates a poorer leaving group (Givens et al., 1993). This may be partially ameliorated by increased  $Mg^{2+}$  coordination with the triphosphate. The general effect of pH on the efficiency and mechanism of the reactions of pHP phototriggers is currently under investigation.

### Rate of release of ATP from pHP-caged ATP

The photorelease of pHP-caged ATP, shown in Fig. 1 B, occurs from the triplet-excited state of the *p*-hydroxyphenacyl chromophore through an intramolecular displacement of ATP with neighboring group participation of the phenoxy group. Release of ATP is proposed to occur through a spirodienedione intermediate formed when the excited triplet undergoes intramolecular displacement of ATP and is subsequently hydrolyzed to provide the *p*-hydroxyphenylacetic acid by-product (Park and Givens, 1997). The rate constant for release was estimated at  $2 \cdot 10^8$  s<sup>-1</sup> from diffusion-limited Stern-Volmer quenching of the reaction, which is in accord with our recent studies on pHP derivatives of oligopeptides and excitatory amino acids (Givens et al., 2000). These results have now been complemented by the FTIR measurements (Fig. 2), which demonstrate directly the appearance of the photoproduct ATP

within less than 1  $\mu$ s and corroborate the proposed photolytic reaction mechanism. Recently, a singlet mechanism involving an excited-state prototropic shift to a reactive enol tautomer was proposed (Zhang et al., 1999). In contrast, current studies in one of our laboratories (Givens et al., 2000) have established the intermediacy of the triplet state in this reaction. Unfortunately, attempts to observe the intermediate spirodienedione by time-resolved FTIR were not successful, probably because of the short lifetime of the spiro intermediate in the highly nucleophilic media and the limited time resolution of the FTIR measurements. The intermediacy of the spirodienedione, therefore, cannot be made on the basis of the present study.

### Desyl-caged ATP

Desyl-caged ATP is similar to DMB-caged ATP, except that it lacks the two methoxy groups. The two methoxy groups serve as a spectroscopic marker that allowed determination of the rate constant of ATP release of  $k > 10^5$  s<sup>-1</sup> for DMB-caged ATP (Corrie and Trentham, 1992). For the aforementioned reasons, this is not possible for desyl-caged ATP, and no information about the rate constant of ATP release is available for this compound. We have obtained transient electrical currents similar to those shown in Fig. 3 after activation of the  $Na^+, K^+$ -ATPase with desyl-caged ATP (data not shown). The magnitude of the currents depends on the concentration of unphotolyzed desyl-caged ATP present in the solution together with the released ATP, demonstrating competitive inhibition of the enzyme by desyl-caged ATP. The currents were approximately two to five times smaller than with NPE-caged ATP but displayed a rapid rise ( $\tau \leq 3$  ms) at pH 6.2, 7.0, and 7.4. This suggests that ATP is released rapidly from desyl-caged ATP in the physiological pH range and can be used for the activation of ATP-dependent enzymes. However, the low photolytic efficiency means a significant limitation on its use.

### Competitive inhibition of $Na^+, K^+$ -ATPase by pHP-caged ATP

Based on previous experience with NPE-caged ATP (Forbush, 1984; Fendler et al., 1985), we used competitive inhibition by pHP-caged ATP as a working hypothesis. This is clearly supported by the fluorescence signal after preincubation with caged ATP (Fig. 5): the rise time is increased but the amplitude remains the same. In addition, the validity of this concept is shown by the kinetic analysis using a kinetic model based on competitive inhibition. If pHP-caged ATP would bind to a site different from the ATP binding site (as required by uncompetitive or noncompetitive inhibition), we would not be able to explain the concentration dependence of the electrical signal with this model.

Values for the dissociation constant of caged ATP ( $K_c$ ) may be calculated from the rate constants  $k_c^+$  and  $k_c^-$  ( $K_c = k_c^-/k_c^+$ ) for caged ATP binding and dissociation, respectively, as determined by the fitting procedure described below. Using these values (Table 4), we obtained dissociation constants for pHP-caged ATP at pH 6.2, 7.0, and 7.4 of 41, 22, and 18  $\mu\text{M}$ , respectively. This represents a much smaller affinity than that for ATP, which in this pH range has a dissociation constant of  $K_a = k_a^-/k_a^+ \sim 5 \mu\text{M}$  (see Table 4). Further support for competitive binding of pHP-caged ATP comes from the fluorescence measurements. As shown in Fig. 5, preincubation of the enzyme with pHP-caged ATP slows down the exponential rise in the fluorescence of RH421-labeled ATPase used to monitor the conformational changes in the enzyme.

The competitive binding of ATP and NPE-caged ATP to the  $\text{Na}^+, \text{K}^+$ -ATPase has been described as a rapid NPE-caged ATP preequilibrium (Fendler et al., 1993; Clarke et al., 1998). This is apparently not the case for pHP-caged ATP, because preincubation with pHP-caged ATP yields a result different from that of the simultaneous addition of NPE-caged ATP and ATP. In contrast, binding and dissociation of pHP-caged ATP have to be much slower than those of ATP because 1) fast binding of pHP-caged ATP would slow down the kinetics of both the preincubation and the simultaneous addition experiment and 2) fast dissociation of pHP-caged ATP would also permit fast kinetics in the preincubation experiment. Therefore, the reciprocal relaxation times found after preincubation with pHP-caged ATP (Table 2) can be taken directly as an approximation for the rate constant for dissociation of pHP-caged ATP from the  $\text{Na}^+, \text{K}^+$ -ATPase. This reaction proceeds with rate constants of  $\sim 55 \text{ s}^{-1}$  at pH 6.2 and  $\sim 30 \text{ s}^{-1}$  at pH 7.4, i.e., somewhat faster at acidic pH.

Slow caged ATP dissociation can also account for the decrease in the peak currents at high caged ATP concentrations (Fig. 4). The effect is most pronounced at pH 6.2. Therefore, in the following argument we will use values determined at pH 6.2. The rise and decay of the peak current with increasing pHP-caged ATP concentration is brought

**TABLE 4** Rate constants (at  $T = 24^\circ\text{C}$ ) of the kinetic model shown in Fig. 1, as determined by the fit

		pH 6.2 ( $n = 2$ )	pH 7.0 ( $n = 3$ )	pH 7.4 ( $n = 1$ )
$k_a^+$	( $\text{M}^{-1}\text{s}^{-1}$ )	$1.0 \cdot 10^7$	$1.2 \cdot 10^7$	$0.76 \cdot 10^7$
$k_a^-$	( $\text{s}^{-1}$ )	50 (fix)	50 (fix)	50 (fix)
$k_c^+$	( $\text{M}^{-1}\text{s}^{-1}$ )	$0.13 \cdot 10^7$	$0.14 \cdot 10^7$	$0.18 \cdot 10^7$
$k_c^-$	( $\text{s}^{-1}$ )	53	31	34
$k_p$	( $\text{s}^{-1}$ )	419	212	383
$k_{12}$	( $\text{s}^{-1}$ )	316	706	266
$k(\text{E}_1\text{ATP} \rightarrow \text{E}_2\text{P})$	( $\text{s}^{-1}$ )	180	163	156

The values are averages of  $n$  experiments,  $k(\text{E}_1 \rightarrow \text{E}_2\text{P})$  is an effective rate constant calculated according to  $k^{-1}(\text{E}_1 \rightarrow \text{E}_2\text{P}) = k_p^{-1} + k_{12}^{-1}$ . A fixed value of  $k_a^- = 50 \text{ s}^{-1}$  was used for the ATP dissociation rate constant.

about by two competing effects: 1) the formation of the phosphointermediate  $\text{E}_2\text{P}$  (see Fig. 7) is accelerated by increasing concentrations of released ATP, but 2) the ATP-binding sites are blocked by slowly dissociating pHP-caged ATP. Up to a caged ATP concentration of  $\sim 100 \mu\text{M}$  (corresponding to  $\sim 40 \mu\text{M}$  released ATP), acceleration by effect 1) dominates the electrical signal, leading to the rise of the peak currents observed in Fig. 4. At  $100 \mu\text{M}$  caged ATP concentration,  $\sim 65\%$  of the enzyme has bound pHP-caged ATP in its ATP-binding site. Thereafter, any further increase in caged ATP concentration results in a concomitant increase in the blocking of the ATP-binding sites by pHP-caged ATP, which in turn decreases the peak currents (see Fig. 4).

### Fit with the kinetic model

Because ATP is rapidly photoreleased from pHP-caged ATP at physiological pH, this caged derivative is well suited for the investigation of rapid reactions in the reaction cycle of the  $\text{Na}^+, \text{K}^+$ -ATPase. Complications arise from the competitive binding of pHP-caged ATP and from its slow dissociation from the  $\text{Na}^+, \text{K}^+$ -ATPase. We have therefore analyzed the currents obtained after a photolytic concentration jump on the basis of the kinetic model shown in Fig. 7, which takes into account interaction of the enzyme with ATP and caged ATP. The differential equations of this model were numerically solved and simultaneously fitted to the current traces obtained at different pH values and ATP concentrations.

Of the two different release models for pHP-caged ATP tested, only the “no release in site” model was successful in reproducing the data, i.e., caged ATP bound to the  $\text{Na}^+, \text{K}^+$ -ATPase is not photolyzed. Interestingly, for NPE-caged ATP and  $\text{Na}^+, \text{K}^+$ -ATPase from eel electric organ, the two models were equally successful (Fendler et al., 1994), while

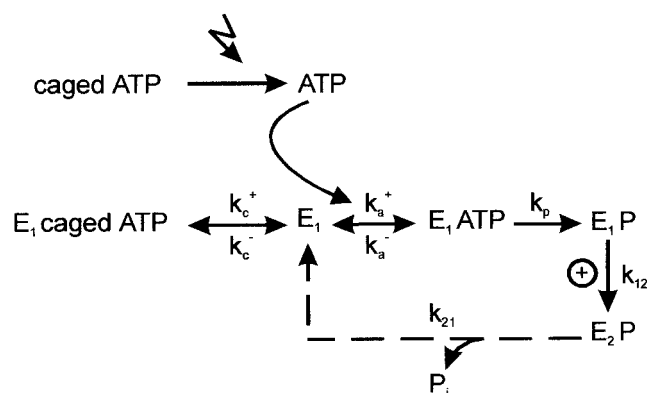


**FIGURE 7** Kinetic model for the  $\text{Na}^+, \text{K}^+$ -ATPase and its activation, using caged ATP. The dephosphorylation reaction is assumed to be slow. Therefore, decay of  $\text{E}_2\text{P}$  and formation of  $\text{E}_1$  were combined into a single slow reaction with a rate constant  $k_{21}$ .

the  $F_0F_1$ -ATPase is activated from NPE-caged ATP via a "release in site" mechanism (unpublished observation). Possibly the structure of the binding site of the  $\text{Na}^+, \text{K}^+$ -ATPase is such that it stabilizes the ATP as well as the hydrophobic cage moiety in such a way that dissociation of the leaving group can no longer occur efficiently. Alternatively, if the site is hydrophobic, it may shift the absorption maximum of the pHP group to a shorter wavelength, making it less capable of absorbing the incident light.

The kinetic parameters determined by the fit at the different pH values are compiled in Table 4. Note that the values for  $k_p$  and  $k_{12}$  have to be regarded with caution. These rate constants have similar values and are therefore highly correlated. This explains the large variation for these parameters in the table. On the other hand, the apparent rate constant of the combined process  $k(\text{E}_1\text{ATP} \rightarrow \text{E}_2\text{P})$  is well defined; this is also given in the table. This rate constant is interesting because it can be directly compared to the rate constant obtained from the fluorescence measurements  $k_{\text{max}}$  (Table 1), which also corresponds to the reaction  $\text{E}_1\text{ATP} \rightarrow \text{E}_2\text{P}$ .

### The rate constants

The values given in Table 4 compare well with the fluorescence data at different pHs. The fit using the complete model supports the conclusion drawn from the fluorescence measurements, namely that the dissociation rate constant of pHP-caged ATP is rather low. The rate constant  $k_{\text{max}}$  corresponds to the two-step reaction  $\text{E}_1\text{ATP} \rightarrow \text{E}_2\text{P}$  and has to be compared with the corresponding rate constant in Table 4. Good agreement is also found in this case.

These results, obtained by two independent methods, demonstrate that at pH 6.2–7.4 and at 24°C, both the phosphorylation and the  $\text{E}_1\text{P} \rightarrow \text{E}_2\text{P}$  conformational transition are rapid reactions with rate constants of 200  $\text{s}^{-1}$  or more. Rate constants were previously reported for the  $\text{E}_1\text{P} \rightarrow \text{E}_2\text{P}$  transition at 24°C ranging from 29  $\text{s}^{-1}$  (Stürmer et al., 1991) to 1400  $\text{s}^{-1}$  (Hobbs et al., 1985; Fendler et al., 1993). This and the former value have been corrected for temperature, using an activation energy of 80 kJ/mol. It was speculated that the discrepancy between these two values was due to a rate-limiting slow release of ATP from NPE-caged ATP or to the choice of different pH values. The present results from pHP-caged ATP suggest that the low values reported for the rate constant of the  $\text{E}_1\text{P} \rightarrow \text{E}_2\text{P}$  transition are most likely incorrect and that this reaction has a rate constant of  $>270 \text{ s}^{-1}$  (24°C) in the pH range 6.2–7.0. Values higher than 270  $\text{s}^{-1}$  are difficult to exclude on the basis of our electrical or RH421 fluorescence measurements because phosphorylation  $\text{E}_1\text{ATP} \rightarrow \text{E}_1\text{P}$  and the conformational transition  $\text{E}_1\text{P} \rightarrow \text{E}_2\text{P}$  take place in series and are difficult to discriminate. Here a rigorous comparison with time-resolved measurements of phosphoenzyme formation is required.

## APPENDIX

The kinetic model of Fig. 7 is described by the following differential equations:

$$\begin{aligned} \frac{d[\text{E}_1\text{cagedATP}]}{dt} &= -[\text{E}_1\text{cagedATP}] \cdot k_c^- \\ &\quad + [\text{E}_1] \cdot k_c^+ \cdot (1 - \eta) \cdot [\text{cagedATP}] \\ \frac{d[\text{E}_1]}{dt} &= -[\text{E}_1] \cdot (k_a^+ \cdot \eta \cdot [\text{cagedATP}] \\ &\quad + k_c^+ \cdot (1 - \eta) \cdot [\text{cagedATP}]) \\ &\quad + [\text{E}_1\text{cagedATP}] \cdot k_c^- + [\text{E}_1\text{ATP}] \cdot k_a^- + [\text{E}_2\text{P}] \cdot k_{21} \\ \frac{d[\text{E}_1\text{ATP}]}{dt} &= -[\text{E}_1\text{ATP}] \cdot (k_a^- + k_p) \\ &\quad + [\text{E}_1] \cdot k_a^+ \cdot \eta \cdot [\text{cagedATP}] \\ \frac{d[\text{E}_1\text{P}]}{dt} &= -[\text{E}_1\text{P}] \cdot k_{12} + [\text{E}_1\text{ATP}] \cdot k_p \\ \frac{d[\text{E}_2\text{P}]}{dt} &= -[\text{E}_2\text{P}] \cdot k_{21} + [\text{E}_1\text{P}] \cdot k_{12} \end{aligned}$$

The electrogenic step is assumed to be the  $\text{E}_1\text{P} \rightarrow \text{E}_2\text{P}$  transition. The current generated by the enzyme  $I_p(t)$  is given by (scaling parameter omitted)

$$I_p(t) = [\text{E}_1\text{P}] \cdot k_{12}$$

For calculation of the measured current  $I(t)$  the capacitive coupling of the membrane fragments to the planar bilayer has to be taken into account (Fendler et al., 1993). Assuming a nonconducting lipid bilayer, we obtain the following two differential equations:

$$\begin{aligned} \frac{dU_m}{dt} + U_m k_0 &= I_p(t) \\ I(t) &= Y_{\text{norm}} \frac{dU_m}{dt} \end{aligned}$$

Here  $k_0$  is the reciprocal system time constant, which is determined exclusively by the electrical properties of the compound membrane (Fendler et al., 1993).  $Y_{\text{norm}}$  is a normalization constant.

Assuming immediate release of ATP from caged ATP, the initial conditions at  $t = 0$  after the photolyzing light flash are given by

$$\begin{aligned} [\text{E}_1\text{cagedATP}]_0 &= \left( \frac{(1 - \eta_{\text{in}})c}{c + k_c^-/k_c^+} \right) \\ [\text{E}_1]_0 &= \left( \frac{k_c^-/k_c^+}{c + k_c^-/k_c^+} \right) \\ [\text{E}_1\text{ATP}]_0 &= \left( \frac{\eta_{\text{in}}c}{c + k_c^-/k_c^+} \right) \end{aligned}$$

$[\text{E}_1\text{P}]_0$  and  $[\text{E}_2\text{P}]_0 = 0$ ;  $c$  is the concentration of caged ATP before the light flash. The fraction of ATP released in solution is  $\eta$ ; that released in the

binding site is  $\eta_{in}$ .  $\eta$  is calculated from the UV light intensity, using the parameters given in Table 3. For the “release in site” model  $\eta_{in} = \eta$ ; for the “no release in site” model  $\eta_{in} = 0$ .

We thank J. E. T. Corrie for providing the absorption spectrum of DMB-caged ATP, and A. Schacht and E. Grell for preparation of the  $\text{Na}^+, \text{K}^+$ -ATPase. Samples of pHP-caged ATP were initially supplied by Dr. Chan-Ho Park.

RSG thanks the National Science Foundation (NSF/OSR-9255223) and the University of Kansas General Research Fund for financial support.

## REFERENCES

- Barabas, K., and L. Keszthelyi. 1984. Temperature dependence of ATP release from “caged” ATP. *Acta Biochim. Biophys. Acad. Sci. Hung.* 19:305–309.
- Barth, A., J. E. T. Corrie, M. J. Gradwell, Y. Maeda, W. Mantele, T. Meier, and D. R. Trentham. 1997. Time-resolved infrared spectroscopy of intermediates and products from photolysis of 1-(2-nitrophenyl)ethyl phosphates—reaction of the 2-nitrosoacetophenone byproduct with thiols. *J. Am. Chem. Soc.* 119:4149–4159.
- Barth, A., K. Hauser, W. Mantele, J. E. T. Corrie, and D. R. Trentham. 1995. Photochemical release of ATP from caged ATP studied by time-resolved infrared spectroscopy. *J. Am. Chem. Soc.* 117:10311–10316.
- Borlinghaus, R., H. J. Apell, and P. Läuger. 1987. Fast charge translocations associated with partial reactions of the Na, K-pump. I. Current and voltage transients after photochemical release of ATP. *J. Membr. Biol.* 97:161–78.
- Clarke, R. J., D. J. Kane, H. J. Apell, M. Roudna, and E. Bamberg. 1998. Kinetics of  $\text{Na}^+$ -dependent conformational changes of rabbit kidney  $\text{Na}^+, \text{K}^+$ -ATPase. *Biophys. J.* 75:1340–1353.
- Colthup, N. B., L. H. Daly, and S. E. Wiberley. 1975. Introduction to Infrared and Raman Spectroscopy. Academic Press, New York.
- Cornelius, F., N. U. Fedosova, and I. Klodos. 1998.  $\text{E}_2\text{P}$  phosphoforms of  $\text{Na}, \text{K}$ -ATPase. II. Interaction of substrate and cation-binding sites in  $\text{P}_i$  phosphorylation of  $\text{Na}, \text{K}$ -ATPase. *Biochemistry.* 37:16686–16696.
- Corrie, J. E. T., and D. R. Trentham. 1992. Synthetic, mechanistic, and photochemical studies of phosphate esters of substituted benzoin. *J. Chem. Soc.* 1:2409–2417.
- Corrie, J. E. T., and D. R. Trentham. 1993. Caged nucleotides and neurotransmitters. In *Biological Applications of Photochemical Switches*. H. Morrison, editor. John Wiley and Sons, New York. 243–305.
- Fendler, K., E. Grell, and E. Bamberg. 1987. Kinetics of pump currents generated by the  $\text{Na}^+, \text{K}^+$ -ATPase. *FEBS Lett.* 224:83–88.
- Fendler, K., E. Grell, M. Haubs, and E. Bamberg. 1985. Pump currents generated by the purified  $\text{Na}^+, \text{K}^+$ -ATPase from kidney on black lipid membranes. *EMBO J.* 4:3079–3085.
- Fendler, K., K. Hartung, G. Nagel, and E. Bamberg. 1998. Investigation of charge translocation by ion pumps and carriers using caged substrates. *Methods Enzymol.* 291:289–306.
- Fendler, K., S. Jaruschewski, J. P. Froehlich, W. Albers, and E. Bamberg. 1994. Electrogenic and electroneutral partial reactions in  $\text{Na}^+, \text{K}^+$ -ATPase from eel electric organ. In *The Sodium Pump*. E. Bamberg and W. Schoner, editors. Steinkopf, Darmstadt. 495–506.
- Fendler, K., S. Jaruschewski, A. Hobbs, W. Albers, and J. P. Froehlich. 1993. Pre-steady-state charge translocation in  $\text{Na}, \text{K}$ -ATPase from eel electric organ. *J. Gen. Physiol.* 102:631–666.
- Forbush, B. d. 1984.  $\text{Na}^+$  movement in a single turnover of the Na pump. *Proc. Natl. Acad. Sci. USA.* 81:5310–5314.
- Givens, R. S., and C. H. Park. 1996. *p*-Hydroxyphenacyl ATP—a new phototrigger. *Tetrahedron Lett.* 37:6259–6262.
- Givens, R. S., S. A. Philip, L. Matuszewski, L. W. I. Kueper, J. Xue, and T. Fister. 1993. Photochemistry of phosphate esters:  $\alpha$ -keto phosphates as a photoprotecting group for caged phosphate. *J. Am. Chem. Soc.* 115:6001–6012.
- Givens, R. S., J. F. W. Weber, P. G. Conrad, G. Orosz, S. L. Donahue, and S. A. Thayer. 2000. New phototriggers 9: *p*-hydroxyphenacyl as a C-terminal photoremovable protecting group for oligopeptides. *J. Am. Chem. Soc.* 122:2687–2697.
- Givens, R. S., J. F. W. Weber, A. H. Jung, and C.-H. Park. 1998. New photoprotecting groups: desyl and *p*-hydroxyphenacyl phosphate and carboxylate esters. *Methods Enzymol.* 291:1–29.
- Gropp, T., N. Brustovetsky, M. Klingenberg, V. Muller, K. Fendler, and E. Bamberg. 1999. Kinetics of electrogenic transport by the ADP/ATP carrier. *Biophys. J.* 77:714–726.
- Hauser, K. 1994. Zeitaufgelöste und statische Infrarotuntersuchungen an photolabilen ATP Derivaten. Diploma. Albert-Ludwigs-Universität, Freiburg, Germany.
- Hobbs, A. S., R. W. Albers, and J. P. Froehlich. 1985. Quenched-flow determination of the  $\text{E}_1\text{P}$  to  $\text{E}_2\text{P}$  transition rate constant in electric organ  $\text{Na}, \text{K}$ -ATPase. In *The Sodium Pump*. I. Glynn and C. Ellory, editors. The Company of Biologists, Cambridge. 355–361.
- Jorgensen, P. L. 1974a. Isolation of  $(\text{Na}^+ + \text{K}^+)\text{-ATPase}$ . *Methods Enzymol.* 32:277–290.
- Jorgensen, P. L. 1974b. Purification and characterization of  $(\text{Na}^+ + \text{K}^+)\text{-ATPase}$ . 3. Purification from the outer medulla of mammalian kidney after selective removal of membrane components by sodium dodecylsulfate. *Biochim. Biophys. Acta.* 356:36–52.
- Kane, D. J., K. Fendler, E. Grell, E. Bamberg, K. Taniguchi, J. P. Froehlich, and R. J. Clarke. 1997. Stopped-flow kinetic investigations of conformational changes of pig kidney  $\text{Na}^+, \text{K}^+$ -ATPase. *Biochemistry.* 36:13406–13420.
- Kane, D. J., E. Grell, E. Bamberg, and R. J. Clarke. 1998. Dephosphorylation kinetics of pig kidney  $\text{Na}^+, \text{K}^+$ -ATPase. *Biochemistry.* 37:4581–4591.
- Kaplan, J. H., B. d. Forbush, and J. F. Hoffman. 1978. Rapid photolytic release of adenosine 5'-triphosphate from a protected analogue: utilization by the  $\text{Na}, \text{K}$  pump of human red blood cell ghosts. *Biochemistry.* 17:1929–1935.
- Mardh, S., and O. Zetterqvist. 1974. Phosphorylation and dephosphorylation reactions of bovine brain  $(\text{Na}^+ - \text{K}^+)\text{-stimulated}$  ATP phosphohydrolase studied by a rapid mixing technique. *Biochim. Biophys. Acta.* 350:473–483.
- Park, C. H., and R. S. Givens. 1997. New photoactivated protecting groups. 6. *p*-Hydroxyphenacyl: a phototrigger for chemical and biochemical probes. *J. Am. Chem. Soc.* 119:2453–2463.
- Sokolov, V. S., H. J. Apell, J. E. Corrie, and D. R. Trentham. 1998. Fast transient currents in  $\text{Na}, \text{K}$ -ATPase induced by ATP concentration jumps from the  $\text{P}_3$ -[1-(3', 5'-dimethoxyphenyl)-2-phenyl-2-oxo]ethyl ester of ATP. *Biophys. J.* 74:2285–2298.
- Stürmer, W., R. Buhler, H. J. Apell, and P. Lauger. 1991. Charge translocation by the  $\text{Na}, \text{K}$ -pump. II. Ion binding and release at the extracellular face. *J. Membr. Biol.* 121:163–176.
- Thirlwell, H., J. E. Corrie, G. P. Reid, D. R. Trentham, and M. A. Ferenczi. 1994. Kinetics of relaxation from rigor of permeabilized fast-twitch skeletal fibers from the rabbit using a novel caged ATP and apyrase. *Biophys. J.* 67:2436–2447.
- Walker, J. W., P. R. Gordon, J. A. McCray, and D. R. Trentham. 1988. Photolabile 1-(2-nitrophenyl)ethyl phosphate esters of adenine nucleotide analogues. Synthesis and mechanism of photolysis. *J. Am. Chem. Soc.* 110:7170–7177.
- Yuzawa, T., C. Kato, M. W. George, and H. Hamaguchi. 1994. Nanosecond time-resolved infrared spectroscopy with a dispersive scanning spectrometer. *Appl. Spectrosc.* 48:684–690.
- Zhang, K., J. E. T. Corrie, V. R. N. Munasinghe, and P. Wan. 1999. Mechanism of photosolvolytic rearrangement of *p*-hydroxyphenacyl esters: evidence for excited-state intramolecular proton transfer as the primary photochemical step. *J. Am. Chem. Soc.* 121:5625–5632.